Differential and Age Dependent Expression of Specific Sialoglycans on HeLa Cells -Revealed by Direct Fluorescent Glycan Labeling

Zhengliang L Wu[1*], Anthony D Person[1], Andrew J. Burton[2], Ravinder Singh[1], Barbara Burroughs[1], Dan Fryxell[1], Timothy J. Tatge[1], Timothy Manning[1], Guoping Wu[1], Karl A.D. Swift[2], Vassili Kalabokis[1]

[1]Bio-techne, R&D Systems, Inc. 614 McKinley Place N.E. Minneapolis, MN, 55413, USA

[2]Bio-Techne, The Watkins Building, Atlantic Road, Avonmouth, Bristol, BS11 9QD, UK.

*Correspondence: Phone: 612-656-4544. Email: leon.wu@bio-techne.com,

Abstract

Cells are covered with sialoglycans. The expression and distribution of specific sialoglycans on cell surface are important for various cellular functions. Imaging these glycans is essential to elucidate their biological roles. Here, utilizing enzymatic incorporation of orthogonal sialic acids, especially fluorophore-conjugated sialic acids, dubbed as direct fluorescent glycan labeling (DFGL), we report the imaging of N- and O-glycans and particularly tumor specific sialyl T antigen on HeLa cells. It is found that while Core-1 O-glycans are relatively evenly distributed on cells, N-glycans expression tend to be more peripheral. More interestingly, the expression of sialyl T antigen displays random and sporadic patterns that likely are age and stress dependent, suggesting that sialyl T antigen expression is not an immediate outcome of direct genetic mutation but rather arises from disordered post-translational machinery. In technique side, DFGL not only allows covalently labeling of sialoglycans on intact glycoproteins with variety of fluorescent dyes, but also allows imaging different sialoglycans simultaneously without cross staining. With the unprecedented convenience and specificity, we believe that technique like DFGL will transform the research on glycoscience.

Introduction

Sialoglycan refers to glycans that are sialylated. The most common sialoglycans are N-glycans that are linked to asparagine residues [1] and O-Glycans that are linked to serine/threonine residues [2]. They are commonly found on cell surface, and involved in cell-cell, cell-extracellular matrix, and cell-pathogen interactions, and therefore play important roles in cell growth, differentiation and migration, innate immunity, and pathogenesis [3-8]. They bind to numerous selectins expressed on mammalian cells [9] and function as binding targets for a large number of pathogenic organisms and their toxins [10,11]. They are involved in cancer malignancy and inflammation, and therefore are potential targets for therapeutic and diagnostic intervention [12-15]. For their important biological functions and therapeutic and diagnostic applications, specific sialoglycan imaging or detection is especially valuable [16-18].

Sialylation of N-glycans and O-glycans is accomplished by a number of sialyltransferases [19] (Fig. 1**A** and 1**B**). N-glycan sialylation typically occurs on Gal residues and is mediated by the N-glycan specific α-2,6-sialyltransferase 1 (ST6Gal1) [20]. O-glycan synthesis is initiated with an O-GalNAc residue that can be elongated to Core-1 O-glycan (T antigen, Galβ1,3-GalNAc-O-S/T) [21] that can be further sialylated by the O-glycan specific α-2,3-sialyltransferase 1 and 2 (ST3Gal1 and ST3Gal2) to generate sialyl-T antigen (sT antigen, Siaα2,3-Galβ1-3GalNAc-O-S/T) [22,23]. O-GalNAc residue can also be directly sialylated at C-6 by a family of α-N-acetylgalactosaminide α-2,6-sialyltransferases (ST6GalNAc). ST6GalNAc4 is strictly active on sT antigen and responsible for disialylated T antigen expression [24].

Despite the abundance of sialoglycans and their important biological functions, research on these glycans was hampered for the lack of high affinity [25] and specific [26-28] binding reagents. The emerge of click chemistry [29] and metabolic glycan labeling using clickable carbohydrate [30-34] made generic glycan imaging possible. Subsequently, enzymatic glycan labeling using clickable sugars made some specific glycan imaging feasible [35-40] (Method I in Fig. 1C). However, specific imaging of sialoglycans is still a big challenge. A possible reason for this difficulty is that sialoglycans are usually on cell surface and fixation of cells usually renders these glycans not accessible to labeling glycosyltranserases.

Recently, probing or labeling N-glycans and sT antigen via direct incorporation of biotinylated sialic acids have been reported, respectively, via ST6Gal1 [41] and ST6GalNAc4 [42] (Method II in Fig. 1C). Here, we especially describe the specific imaging of these glycans on HeLa cells via Direct Fluorescent Glycan Labeling (DFGL) where fluorophore-conjugated sialic acids are directly enzymatically incorporated (Method III in Fig. 1C). HeLa cells are derived from human cervical cancer cells [43] and are genetically stable [44]. HeLa cells are also known to express CA125, a glycoprotein cancer marker that carries T/sT antigens [45]. By comparing the images of N-glycan and T/sT antigens, we found that these glycans on HeLa cells have different localization, and, more interestingly, the expression of sT antigen on HeLa cells displays random and sporadic patterns that are likely age and stress dependent.

Results

Fluorophore Conjugated Sialic Acids can be Directly Introduced to Glycoprotein by Various Sialyltransferases

CMP-sialic acids (CMP-SA) with fluorophore directly conjugated to sialic acids were synthesized by incubating equal amounts of CMP-azido-sialic acid with various alkyne fluorophores via copper (I)-catalyzed azide-alkyne cycloaddition [46]. Alexa Fluor® 555 conjugated CMP-SA was first tested on fetal bovine fetuin using various sialyltransferases. The labeling reactions were separated on SDS-PAGE and directly imaged with a fluorescent imager and a regular protein gel imager (Fig. 2A, 2B and 2C.The uncropped images are displayed in Supplemental Fig. 1). Indeed, Alexa Fluor® 555 conjugated sialic acid was directly introduced to asialofetuin strongly by ST3Gal1, ST3Gal2 and ST6Gal1, and, weakly by ST6GalNAc1 and ST6GalNAc2. In contrast, the fluorescent sialic acid was directly introduced to fetuin only by ST6GalNAc1, ST6GalNAc2 and ST6GalNAc4. It is clear that ST3Gal1, ST3Gal2, ST6Gal1 showed strict specificity towards asialofetuin and ST6GalNAc4 showed strict specificity towards fetuin, which is consistent to the observation previously achieved with azido-sialic acid [47].

For their strict substrate specificity, ST3Gal1, ST6Gal1 and ST6GalNAc4 were further selected to compare their tolerance on Alexa Fluor® 488, Alexa Fluor® 555 and Cy5 conjugated CMP-SA (Fig. 2D, 2E and 2F). As results, all three dyes were tolerated well by ST3Gal1 and ST6Gal1, but Cy5 was not tolerated by ST6GalNAc4 at all.

Differential Display of Sialoglycans on HeLa Cells

ST3Gal1, ST6Gal1 and ST6GalNAc4 were then selected to image specific sialoglycans on confluent HeLa cells grown in a 96-well plate (Fig. 3). Some cells were pretreated with *C. perfringens* neuraminidase [48] briefly to remove the preexisting α2-3 and α2-6 linked sialic acids before imaging. As results, ST3Gal1 and ST6Gal1 produced strong staining only after the neuraminidase treatment, suggesting that Core-1 O-glycans (or T antigen) and N-glycans were largely sialylated on the HeLa cells. In contrast, ST6GalNAc4 only produced strong staining prior to neuraminidase treatment, indicating the presence of sT antigen on the HeLa cells. Interestingly, while ST3Gal1 and ST6GalNAc4 staining was distributed throughout the cells (Fig. 3B and 3C), ST6Gal1 staining was more peripherally localized (Fig. 3. **F**). For comparison, some cells were also imaged by OGT (Fig. 3. **H**), an enzyme that strictly recognizes intracellular compartments, especially nuclei and cytoplasm [49,50]. Compared to the intracellular staining by OGT, ST6Gal1 clearly stained the cell surface, which became more obvious when HeLa cells were double imaged by ST6Gal1 and OGT (Supplemental Fig. 2). The layer of glycans on the surface of HeLa cells revealed by ST6Gal1 ranged from 5 µm to 20 µm in thickness, which is comparable to that of the glycocalyx of the endothelial cells revealed by electron microscopy [51]. Moreover, in images exhibiting positive staining by ST3Gal1 (Fig. 3. B) and ST6GalNAc4 (Fig. 3.C), some cells were weakly stained or not stained, indicating the variable expression of T/sT antigens by the HeLa cells.

Differential Expression of N- and O-glycans Confirmed by Direct Double Imaging

To confirm that O- and N-glycans have different localization, HeLa cells at different confluence were double imaged by ST3Gal1 and ST6Gal1 (Fig. 4), in which Alexa Fluor® 555 conjugated sialic acid was first introduced by ST3Gal1 followed by the introduction of Alexa Fluor® 488 conjugated sialic acid by ST6Gal1. Again, it was observed that N-glycans revealed by ST6Gal1 were preferentially expressed at the cell edges and Core-1 O-glycans were more centralized and evenly distributed on cells (also see in Supplemental Fig. 3).

It was also noticeable from Fig.4A that N-glycan expression is prominent on protrusions of sub-confluent cells (also see Supplemental Fig.2). To better understand the expression of N-glycans, HeLa cells of increasing confluence were imaged by ST6Gal1 (Supplemental Fig. 4). At about 50% culture confluence, N-glycans already displayed preferential distribution at peripheral positions. It seemed that the N-glycans tend to accumulate at the cell edges during the course of growth possibly for cell attachment and migration. This tendency continued until 100% confluence was reached, in which glycocalyx were merged and condensed to ridges between cells (Fig. 4C and Supplemental Fig.3 D).

Mosaic Expression T/sT antigen and Its Mechanism of Formation

To confirm and better understand the mosaic expression of sT antigen observed in Fig.3C, confluent HeLa cells that were imaged by ST6GalNAc4 were further imaged by OGT to reveal all cell entities (Fig. 5). Again, sT antigen expression varied significantly from cell to cell, with some cells being strongly positive and some cells being almost completely negative.

Occasionally, a positive cell was found to be surrounded by negative cells (circled in Fig. 5B), suggesting that the positive cell be derived from the negative cells, as it is unlikely for a single positive cell being trapped among negative cells during cell division and migration. Mosaic expression of T/sT antigen was also observed on HeLa cells imaged by ST3Gal1 (Supplemental Fig. 5).

HeLa cells are cancerous cells. The expression of sT carbohydrate cancer antigen on HeLa cells is not surprising [45]. However, the mosaic expression of sT antigen is intriguing. Two hypotheses were postulated to explain this phenomenon. The first is that positive cells were derived from negative cells, which is suggested by Fig. 5. The second is that the initial HeLa cell population were heterogeneous and contained positive subpopulation. To test the second hypothesis, HeLa cells from the above experiments were subject to further clonal selection, by which single cells were selected and cultivated under the same conditions for 11-14 days to form individual colonies. When imaged by ST6GalNAc4 at day 11, sT antigen positive cells were sporadically found throughout the colonies but more abundantly around the centers of these colonies (Fig. 6). More sT antigen positive cells were found around the centers of these colonies at day 14 (Supplemental Fig. 6). Since cells around the centers of the colonies are older and more crowded (more stress) than cells at peripheral positions, the above observations together strongly argues that sT antigen positive cells were derived from sT antigen negative cells and the expression is age/stress dependent, which further suggests that sT antigen expression is not due to immediate genetic mutation. Conversely, if sT antigen expression is an immediate outcome of genetic mutations, it should be found on all cells that were descendent from same ancestral cells, which was not the case in Fig.6.

To further test the effect of age/stress, confluent HeLa cells were grown to different time points and imaged for T and sT antigen expression using ST3Gal1 and ST6GalNAc4, respectively (Supplemental Fig. 7). As expected, more positive cells of both T and sT antigens were found on cells of longer incubation time, confirming the hypothesis of age/stress dependence of T/sT antigen expression.

Discussion

In this report, we describe the specific imaging of sialoglycans on HeLa cells and present evidence that different sialoglycans have distinct expression patterns. While O-glycans such as T/sT antigens are more centralized and evenly distributed on cells, N-glycans tend to be localized at peripheral positions. While N-glycans are expressed on all cells, T/sT antigens expression is sporadic and likely age/stress dependent. It is hard to discern the effect of age from stress, as aged cells are more likely to be stressed.

The fact that specific glycan structures can be reproducibly generated by normal cells without templates suggests that the Golgi apparatus has an extremely well-organized structure with the synthetic glycosyltransferases localized in precise order. It is hypothesized that this ordered structure in HeLa cells or pre-cancerous cells is rather fragile and easy to be disrupted under the effects of age and/or stress, leading to premature synthesis of abnormal shortened glycan epitopes.

Cancers were considered as genetic diseases [52]. However, recent work suggests that mutations of oncogenes arise in normal tissues may not necessarily lead to cancer [53]. Direct causes of

cancerous phenotype may need additional factors, such as environmental triggers[54]. Conversely, a cancerous phenotype may not be a direct outcome of genetic mutations. Accordingly, our results on sT antigen imaging strongly argue that its expression is not due to immediate genetic mutation but caused by disrupted posttranslational machinery, which is also supported by the notion that HeLa cells are genomically stable [44]. Recently, glycan cancer antigens have been targeted for cancer immunotherapy [55,56]. A way for imaging or detecting these glycan cancer antigens may help us to better design therapeutic strategies.

The sialoglycans detected in this report are either O-glycans or N-glycans. Their distinct localizations suggest that they are differentially conjugated to glycoproteins on cell surface, and individual glycoproteins may be enriched with one type of glycan but not the other. The distinct localizations also suggest that these glycans may have different functions. For instance, the N-glycans expressed at cell edges could be involved in cell-cell and cell-ECM interactions to facilitate cell adhesion and migration, and the O-glycans displayed on cell surface could be involved in receptor recognition and providing protection from pathogens. Consistently, integrins that are extensively modified with N-glycans are known to be localized at cell edges and to mediate cell-cell and cell-matrix interactions [57], and, mucins that are heavily O-glycosylated are usually expressed on epithelial cell surface where they fulfill a protective role by binding to pathogens [58,59].

In technique side, we reported Direct Fluorescent Glycan Labeling (DFGL) for the first time. DFGL has several advantages over previous methods. First, the method is more convenient and time-saving by involving only a single step of enzymatic reaction prior to cell fixation and imaging. As a method for glycoprotein labeling, it allows direct imaging of an SDS gel under a

fluorescent imager, completely eliminating the time-consuming and error-prone membrane blotting process. Second, this method is more suitable for live cell imaging by avoiding the toxic copper ion from click chemistry reaction. Third, this method allows double or multiple imaging of different glycans simultaneously without cross-staining of these glycans by avoiding the common intermediate step of biotin-streptavidin reaction. Fourth, since fluorophore is only introduced by enzymatic reaction, the labeling/detection of a certain sialoglycan is more specific and has lower background. In summary, DFGL is a convenient tool for specific sialoglycan detection, labeling and imaging. With DFGL, we believe sialoglycans are no longer the dark matters of life science as referred by pioneers in the field [60].

Material and Methods

CMP-Azido-Sialic acid, UDP-Azido-GlcNAc, Biotinylated Alkyne, DAPI, recombinant human ST3Gal1, ST6Gal1, ST6GalNAc1, ST6GalNAc4, OGT and *C. perfringens* Neuraminidase were from Bio-Techne. Alkyne-Alexa Fluor® 488, alkyne-Alexa Fluor®555, streptavidin-Alexa® Fluor 555, streptavidin-Alexa® Fluor 488 and Click-iT® Biotin DIBO Alkyne were from Thermo Fisher Scientific. Cy5-alkyne, ascorbic acid and all other chemical reagents were from Sigma-Aldrich.

Preparation of fluorescent/biotin conjugated CMP-sialic acid

Fluorophore or biotin conjugated CMP-sialic acids (CMP-SA) were prepared by incubating equivalent amounts of CMP-Azido-Sialic acid and fluorophore or biotin-alkyne conjugates via copper (I)-catalyzed azide-alkyne cycloaddition. The labeled conjugates were then loaded onto a DEAE based ion-exchange column and eluted with a gradient of NaCl elution buffer (150 NaCl, 25 mM Tris at pH 7.5). Biotinylated CMP-SA, Alexa Fluor® 555 conjugated CMP-SA, Alexa Fluor® 488 conjugated CMP-SA, Cy5 conjugated CMP-SA were prepared and purified accordingly and finally concentrated to >0.1 mM in concentration by a speed-vacuum concentrator.

Protein labeling and imaging with fluorophore conjugated CMP-sialic acid

To label glycoproteins with fluorophore-conjugated CMP-SA, 1 to 5 μg of a target protein was mixed with 0.2 nmol fluorophore CMP-SA, 0.2 μg of interested sialyltransferase supplemented with sialyltransferase buffer (25 mM Tris pH7.5, 10 mM $MnCl_2$) to a final volume of 30 μL. The reaction was the incubated at 37°C for 20 minutes. In the case that the preexisting sialic acid of

the glycoprotein needs to be removed, 0.01 ug of *C. perfringens* Neuraminidase was also added into the reaction. The reaction was then separated with SDS-PAGE and the gel was directly imaged with FluorChem M (ProteinSimple, Bio-techne).

Cell Culture

HeLa cells (ATCC # CCL2) were grown in MEM NEAA Earle's Salts (Irvine Scientific, #9130), supplemented with 10% fetal bovine serum (Corning, #35-015-CV), 2 mM L-glutamine, 100 units/mL penicillin and 0.1 mg/mL streptomycin (Sigma-Aldrich, #G6784). Upon confluence, cells were trypsinized and seeded in a 96-well cell culture plate and grown to the desired confluence.

Labeling with clickable carbohydrates using glycosyltransferases

To remove existing sialic acid on cells, 1 µg of *C.p* Neuraminidase was added to each well and incubated for 10 minutes at 37°C. The cells were then washed three times quickly with 150 µL 25 mM Tris pH 7.5, 150 mM NaCl. For labeling using ST3Gal1 or ST6Gal1 or ST6GalNAc1, a mixture of 1 nmol of CMP-Azido-Sialic acid, 1 µg enzyme, 30 µL 25 mM Tris pH 7.5, 150 mM NaCl, 10 mM Mn^{2+}, and 20 µL of conditioned medium was added to each well, and the cells were incubated at 37°C for 20 minutes. For labeling using OGT, a mixture of 1 nmol of UDP-Azido-GlcNAc, 1 µg of the enzyme, 50 µL of the labeling buffer (25 mM MES, 0.5% (w/v) Triton® X-100, 2.5 mM $MgCl_2$, 10 mM $MnCl_2$, 1.25 mM $CaCl_2$ and 0.75 mg/mL of BSA at pH 7.0) was added to each well, and the cells were incubated at 37°C for 60 minutes. After labeling, cells were rinsed with washing buffer (25 mM Tris pH 7.5, 150 mM NaCl) and fixed in 4% paraformaldehyde for 10 minutes at room temperature followed by washing twice with washing

buffer. The cells were then subject to click chemistry reaction by incubating with 0.1 mM Cu^{2+}, 1 mM ascorbic acid and 0.1 mM Biotinylated Alkyne at room temperature for 30 minutes, followed by incubating with 10 µg/mL streptavidin-Alexa® 555 or 488 for 15 minutes.

Direct fluorescent glycan labeling (DFGL) and Labeling with biotin using glycosyltransferases

For DFGL using ST6GalNAc4, a mixture of 0.2 nmol of fluorophore-conjugated CMP-SA, 1 µg of the enzyme, 30 µL labeling buffer and 20 µL of conditioned medium was added to each well, and the cells were incubated for 20 minutes at 37ºC. For DFGL using ST3Gal1 or ST6Gal1, cells in each well were pretreated with 1 µg of *C.p* Neuraminidase at 37ºC for 10 minutes. The cells were then washed three times quickly with 150 µL 25 mM Tris pH 7.5, 150 mM NaCl. Labeling with biotin was achieved by addition of a mixture of 0.2 nmol of fluorophore-conjugated CMP-SA, 1 µg of the enzyme, 30 µL 25 mM Tris pH 7.5, 150 mM NaCl, 10 mM Mn^{2+}, and 20 µL of conditioned medium to each well, and the cells were incubated at 37ºC for 20 minutes. For labeling with biotin-conjugated CMP-SA, substitute fluorophore-conjugated CMP-SA with biotin-conjugated CMP-SA. The cells were then fixed in 4% paraformaldehyde for 10 minutes at room temperature followed by incubating with 10 µg/mL streptavidin-Alexa® 555 or 488 for 15 minutes.

Equipment and Settings

All cell images were captured on an AXIO Observer microscope (ZEISS) with a ZEISS Axiocam 506 mono camera and Zen 2 Pro software. Images were captured simultaneously through different fluorescent channels. Exposure time for each channel ranged from 100 ms to 4000 ms. For best viewing, obtained images from each channel was usually normalized to its highest pixel value.

For taking fluorescent image of SDS gels using FluorChem M, multiple fluorescent channel RGB or single fluorescent channel was selected based on the incorporated fluorescent dyes, and the exposure time was set at Auto.

Author Contributions

Conceptualization, Z.L.W., A.D.P and V.K.; Methodology, Z.L.W., A.J.B.; B.B., R.S., and T.J.T.; K.A.D.S., Investigation, Z.L.W., A.D.P.; Writing – Original Draft, Z.L.W.; Writing – Review & Editing, Z.L.W., A.D.P.; D.F.; T.M. and G.W.; Resources, Z.L.W., A.J.B. T.J.T., K.A.D.S., G.W. and V.K.

Competing Interests

The authors are employee of Bio-techne and there is no competing interests otherwise.

Data availability

The raw data are available upon requests to the corresponding author.

References

1 Stanley, P., Taniguchi, N. & Aebi, M. in *Essentials of Glycobiology* (eds rd *et al.*) 99-111 (2015).

2 Brockhausen, I. & Stanley, P. in *Essentials of Glycobiology* (eds rd *et al.*) 113-123 (2015).

3 Taniguchi, N. & Kizuka, Y. Glycans and cancer: role of N-glycans in cancer biomarker, progression and metastasis, and therapeutics. *Advances in cancer research* **126**, 11-51, doi:10.1016/bs.acr.2014.11.001 (2015).

4 Tabak, L. A. The role of mucin-type O-glycans in eukaryotic development. *Seminars in cell & developmental biology* **21**, 616-621, doi:10.1016/j.semcdb.2010.02.001 (2010).

5 Hollingsworth, M. A. & Swanson, B. J. Mucins in cancer: protection and control of the cell surface. *Nature reviews. Cancer* **4**, 45-60, doi:10.1038/nrc1251 (2004).

6 Spiro, R. G. Protein glycosylation: nature, distribution, enzymatic formation, and disease implications of glycopeptide bonds. *Glycobiology* **12**, 43R-56R (2002).

7 Varki, A. Biological roles of glycans. *Glycobiology* **27**, 3-49, doi:10.1093/glycob/cww086 (2017).

8 Lauc, G., Pezer, M., Rudan, I. & Campbell, H. Mechanisms of disease: The human N-glycome. *Biochimica et biophysica acta* **1860**, 1574-1582, doi:10.1016/j.bbagen.2015.10.016 (2016).

9 Crocker, P. R. *et al.* Siglecs: a family of sialic-acid binding lectins. *Glycobiology* **8**, v (1998).

10 Varki, A. Sialic acids in human health and disease. *Trends in molecular medicine* **14**, 351-360, doi:10.1016/j.molmed.2008.06.002 (2008).

11 Schauer, R. Sialic acids as regulators of molecular and cellular interactions. *Current opinion in structural biology* **19**, 507-514, doi:10.1016/j.sbi.2009.06.003 (2009).

12 Pearce, O. M. & Laubli, H. Sialic acids in cancer biology and immunity. *Glycobiology* **26**, 111-128, doi:10.1093/glycob/cwv097 (2016).

13 Pinho, S. S. & Reis, C. A. Glycosylation in cancer: mechanisms and clinical implications. *Nature reviews. Cancer* **15**, 540-555, doi:10.1038/nrc3982 (2015).

14 Magalhaes, A., Duarte, H. O. & Reis, C. A. Aberrant Glycosylation in Cancer: A Novel Molecular Mechanism Controlling Metastasis. *Cancer cell* **31**, 733-735, doi:10.1016/j.ccell.2017.05.012 (2017).

15 Dube, D. H. & Bertozzi, C. R. Glycans in cancer and inflammation--potential for therapeutics and diagnostics. *Nature reviews. Drug discovery* **4**, 477-488, doi:10.1038/nrd1751 (2005).

16 Schauer, R. Achievements and challenges of sialic acid research. *Glycoconjugate journal* **17**, 485-499 (2000).

17 Chen, X. & Varki, A. Advances in the biology and chemistry of sialic acids. *ACS chemical biology* **5**, 163-176, doi:10.1021/cb900266r (2010).

18 Cummings, R. D. & Pierce, J. M. The challenge and promise of glycomics. *Chemistry & biology* **21**, 1-15, doi:10.1016/j.chembiol.2013.12.010 (2014).

19 Harduin-Lepers, A., Mollicone, R., Delannoy, P. & Oriol, R. The animal sialyltransferases and sialyltransferase-related genes: a phylogenetic approach. *Glycobiology* **15**, 805-817, doi:10.1093/glycob/cwi063 (2005).

20 Weinstein, J., Lee, E. U., McEntee, K., Lai, P. H. & Paulson, J. C. Primary structure of beta-galactoside alpha 2,6-sialyltransferase. Conversion of membrane-bound enzyme to soluble forms by cleavage of the NH2-terminal signal anchor. *The Journal of biological chemistry* **262**, 17735-17743 (1987).

21 Ju, T. & Cummings, R. D. Protein glycosylation: chaperone mutation in Tn syndrome. *Nature* **437**, 1252, doi:10.1038/4371252a (2005).

22 Kitagawa, H. & Paulson, J. C. Cloning of a novel alpha 2,3-sialyltransferase that sialylates glycoprotein and glycolipid carbohydrate groups. *The Journal of biological chemistry* **269**, 1394-1401 (1994).

23 Ju, T. *et al.* Human tumor antigens Tn and sialyl Tn arise from mutations in Cosmc. *Cancer research* **68**, 1636-1646, doi:10.1158/0008-5472.CAN-07-2345 (2008).

24 Harduin-Lepers, A. *et al.* Cloning, expression and gene organization of a human Neu5Ac alpha 2-3Gal beta 1-3GalNAc alpha 2,6-sialyltransferase: hST6GalNAcIV. *The Biochemical journal* **352 Pt 1**, 37-48 (2000).

25 Ambrosi, M., Cameron, N. R. & Davis, B. G. Lectins: tools for the molecular understanding of the glycocode. *Organic & biomolecular chemistry* **3**, 1593-1608, doi:10.1039/b414350g (2005).

26 Sterner, E., Flanagan, N. & Gildersleeve, J. C. Perspectives on Anti-Glycan Antibodies Gleaned from Development of a Community Resource Database. *ACS chemical biology* **11**, 1773-1783, doi:10.1021/acschembio.6b00244 (2016).

27 Glycosciences, N. R. C. U. C. o. A. t. I. a. I. o. G. a. in *Transforming Glycoscience: A Roadmap for the Future The National Academies Collection: Reports funded by National Institutes of Health* (2012).

28 Geisler, C. & Jarvis, D. L. Effective glycoanalysis with Maackia amurensis lectins requires a clear understanding of their binding specificities. *Glycobiology* **21**, 988-993 (2011).

29 Kolb, H. C., Finn, M. G. & Sharpless, K. B. Click Chemistry: Diverse Chemical Function from a Few Good Reactions. *Angewandte Chemie* **40**, 2004-2021 (2001).

30 Codelli, J. A., Baskin, J. M., Agard, N. J. & Bertozzi, C. R. Second-generation difluorinated cyclooctynes for copper-free click chemistry. *Journal of the American Chemical Society* **130**, 11486-11493, doi:10.1021/ja803086r (2008).

31 Baskin, J. M., Dehnert, K. W., Laughlin, S. T., Amacher, S. L. & Bertozzi, C. R. Visualizing enveloping layer glycans during zebrafish early embryogenesis. *Proceedings of the National Academy of Sciences of the United States of America* **107**, 10360-10365, doi:10.1073/pnas.0912081107 (2010).

32 Kizuka, Y. *et al.* High-Sensitivity and Low-Toxicity Fucose Probe for Glycan Imaging and Biomarker Discovery. *Cell chemical biology* **23**, 782-792, doi:10.1016/j.chembiol.2016.06.010 (2016).

33 Hsu, T. L. *et al.* Alkynyl sugar analogs for the labeling and visualization of glycoconjugates in cells. *Proceedings of the National Academy of Sciences of the United States of America* **104**, 2614-2619, doi:10.1073/pnas.0611307104 (2007).

34 Sawa, M. *et al.* Glycoproteomic probes for fluorescent imaging of fucosylated glycans in vivo. *Proceedings of the National Academy of Sciences of the United States of America* **103**, 12371-12376, doi:10.1073/pnas.0605418103 (2006).

35 Griffin, M. E. & Hsieh-Wilson, L. C. Glycan Engineering for Cell and Developmental Biology. *Cell chemical biology* **23**, 108-121, doi:10.1016/j.chembiol.2015.12.007 (2016).

36 Clark, P. M. *et al.* Direct in-gel fluorescence detection and cellular imaging of O-GlcNAc-modified proteins. *Journal of the American Chemical Society* **130**, 11576-11577, doi:10.1021/ja8030467 (2008).

37 Chaubard, J. L., Krishnamurthy, C., Yi, W., Smith, D. F. & Hsieh-Wilson, L. C. Chemoenzymatic probes for detecting and imaging fucose-alpha(1-2)-galactose glycan biomarkers. *Journal of the American Chemical Society* **134**, 4489-4492, doi:10.1021/ja211312u (2012).

38 Zheng, T. *et al.* Tracking N-acetyllactosamine on cell-surface glycans in vivo. *Angewandte Chemie* **50**, 4113-4118, doi:10.1002/anie.201100265 (2011).

39 Mbua, N. E. *et al.* Selective exo-enzymatic labeling of N-glycans on the surface of living cells by recombinant ST6Gal I. *Angewandte Chemie* **52**, 13012-13015, doi:10.1002/anie.201307095 (2013).

40 Wu, Z. L. *et al.* Imaging specific cellular glycan structures using glycosyltransferases via click chemistry. *Glycobiology* **28**, 69-79, doi:10.1093/glycob/cwx095 (2018).

41 Capicciotti, C. J. *et al.* Cell-Surface Glyco-Engineering by Exogenous Enzymatic Transfer Using a Bifunctional CMP-Neu5Ac Derivative. *Journal of the American Chemical Society* **139**, 13342-13348, doi:10.1021/jacs.7b05358 (2017).

42 Wen, L. *et al.* A One-Step Chemoenzymatic Labeling Strategy for Probing Sialylated Thomsen-Friedenreich Antigen. *ACS Cent Sci* **4**, 451-457, doi:10.1021/acscentsci.7b00573 (2018).

43 Scherer, W. F., Syverton, J. T. & Gey, G. O. Studies on the propagation in vitro of poliomyelitis viruses. IV. Viral multiplication in a stable strain of human malignant epithelial cells (strain HeLa) derived from an epidermoid carcinoma of the cervix. *The Journal of experimental medicine* **97**, 695-710 (1953).

44 Adey, A. *et al.* The haplotype-resolved genome and epigenome of the aneuploid HeLa cancer cell line. *Nature* **500**, 207-211, doi:10.1038/nature12064 (2013).

45 Seelenmeyer, C., Wegehingel, S., Lechner, J. & Nickel, W. The cancer antigen CA125 represents a novel counter receptor for galectin-1. *Journal of cell science* **116**, 1305-1318 (2003).

46 Rostovtsev, V. V., Green, L. G., Fokin, V. V. & Sharpless, K. B. A stepwise huisgen cycloaddition process: copper(I)-catalyzed regioselective "ligation" of azides and terminal alkynes. *Angewandte Chemie* **41**, 2596-2599, doi:10.1002/1521-3773(20020715)41:14<2596::AID-ANIE2596>3.0.CO;2-4 (2002).

47 Wu, Z. L., Huang, X., Burton, A. J. & Swift, K. A. Probing sialoglycans on fetal bovine fetuin with azido-sugars using glycosyltransferases. *Glycobiology* **26**, 329-334, doi:10.1093/glycob/cwv109 (2016).

48 Corfield, A. P., Higa, H., Paulson, J. C. & Schauer, R. The specificity of viral and bacterial sialidases for alpha(2-3)- and alpha(2-6)-linked sialic acids in glycoproteins. *Biochimica et biophysica acta* **744**, 121-126 (1983).

49 Wells, L., Vosseller, K. & Hart, G. W. Glycosylation of nucleocytoplasmic proteins: signal transduction and O-GlcNAc. *Science* **291**, 2376-2378 (2001).

50 Wu, Z. L., Tatge, T. J., Grill, A. E. & Zou, Y. Detecting and Imaging O-GlcNAc Sites Using Glycosyltransferases: A Systematic Approach to Study O-GlcNAc. *Cell Chemical biology* **25**, 1-8, doi:http://doi.org/10.1016/j.chemibiol.2018.07.007 (2018).

51 Ebong, E. E., Macaluso, F. P., Spray, D. C. & Tarbell, J. M. Imaging the endothelial glycocalyx in vitro by rapid freezing/freeze substitution transmission electron microscopy. *Arteriosclerosis, thrombosis, and vascular biology* **31**, 1908-1915, doi:10.1161/ATVBAHA.111.225268 (2011).

52 Alexandrov, L. B. *et al.* Signatures of mutational processes in human cancer. *Nature* **500**, 415-421, doi:10.1038/nature12477 (2013).

53 Martincorena, I. *et al.* Somatic mutant clones colonize the human esophagus with age. *Science* **362**, 911-917, doi:10.1126/science.aau3879 (2018).

54 Chanock, S. J. The paradox of mutations and cancer. *Science* **362**, 893-894, doi:10.1126/science.aav5697 (2018).

55 Posey, A. D., Jr. *et al.* Engineered CAR T Cells Targeting the Cancer-Associated Tn-Glycoform of the Membrane Mucin MUC1 Control Adenocarcinoma. *Immunity* **44**, 1444-1454, doi:10.1016/j.immuni.2016.05.014 (2016).

56 Steentoft, C. *et al.* Glycan-Directed Car-T Cells. *Glycobiology*, doi:10.1093/glycob/cwy008 (2018).

57 Hynes, R. O. Integrins: bidirectional, allosteric signaling machines. *Cell* **110**, 673-687 (2002).

58 Hattrup, C. L. & Gendler, S. J. Structure and function of the cell surface (tethered) mucins. *Annual review of physiology* **70**, 431-457, doi:10.1146/annurev.physiol.70.113006.100659 (2008).

59 Linden, S. K. *et al.* MUC1 limits Helicobacter pylori infection both by steric hindrance and by acting as a releasable decoy. *PLoS pathogens* **5**, e1000617, doi:10.1371/journal.ppat.1000617 (2009).

60 Varki, A. Omics: Account for the 'dark matter' of biology. *Nature* **497**, 565, doi:10.1038/497565a (2013).

Figure legends

Figure 1. Sialylation reactions on N-glycans (A) and O-glycans (B) utilized in this report, and, methods of sialoglycan labeling (C). In **A** and **B**, sialylation reactions that are utilized in this report for labeling and imaging are indicated with red arrows. In **C,** three methods are depicted for sialoglycan labeling and imaging. In method I, azido-sialic acid is incorporated into sialoglycans, followed by click chemistry reaction to attach a biotin molecule and then labeled by fluorophore-conjugated streptavidin. In method II, biotinylated sialic acid is incorporated into sialoglycans and then labeled by fluorophore-conjugated streptavidin. Method III is named as Direct Fluorescent Glycan Labeling (DFGL) where sialoglycans are labeled by direct incorporation of fluorophore-conjugated sialic acid. Neu, neuraminidase; STs, sialyltransferases; CMP, cytidine monophosphate**.** Full-length gels are presented in Supplementary Fig. 1.

Figure 2. Fluorophore conjugated CMP-Sialic acids are tolerated by various sialyltransferases. **A** (TCE image), **B** and **C** (fluorescent images with different contrast) were images for a same SDS-PAGE gel, where Alexa Fluor® 555 labeled fetuin (F) or asialofetuin (AF) via indicated sialyltransferases was separated. **D** (TCE image), **E** and **F** (fluorescent images of different contrast) were images for a same SDS-PAGE gel, where Alexa Fluor® 488, 555 and Cy5 labeled F or AF with indicated sialyltransferases were separated. 31, ST3Gal1; 32, ST3Gal2; 34, ST3Gal4; 61, ST6Gal1; 6A1, ST6GalNAc1; 6A2, ST6GalNAc2; 6A4, ST6GalNAc4. Same amounts of F or AF (2.5 µg) was loaded into each lane in both **A** and **D**; however, due to the presence of multiple benzene rings in Alexa-Fluor® dyes, Alexa Fluor® 488 and 555 labeled proteins showed significantly increased band intensities in TCE gels. The *C.P neuraminidase* used for AF preparation in panel **A** was not removed, as it showed no glycosidase activity on the introduced orthogonal sialic acids. MM, molecular marker.

Figure 3. N- and O-glycans exhibit different localization on HeLa Cells. Confluent HeLa cells were imaged by ST3Gal1 (**A** and **B**), ST6GalNAc4 (**C** and **D**), ST6Gal1 (**E** and **F**) before (**A**, **C**, **E**) and after (**B**, **D, F**) *C.p. neuraminidase* treatment using CMP-azido-sialic acid. The cells were stained by ST3Gal1 and ST6Gal1 only after *C. perfringens* neuraminidase treatment, suggesting that both Core-1 O-glycan (T antigen) and N-glycan were highly sialylated on these cells. On the contrary, sT antigen was only stained by ST6GalNAc4 prior to *C. p* neuraminidase treatment (**C**). While sT antigen revealed in panels **B** and **C** evenly distributed on cell surface, N-glycans revealed in panel **F** showed a more peripheral localization. Additionally, not all cells in panel **B** and **C** were equally positive for sT antigen. For comparison, intracellular contents were stained by OGT in **H** using UDP-azido-GlcNAc. All staining was achieved through Alexa Fluor® 555 via click chemistry and streptavidin-biotin binding. Nuclei were stained in blue with DAPI.

Figure 4. Differential Expression of N-glycans and Core-1 O-glycans Revealed by Double Imaging. HeLa cells at sub-confluence (**A** and **B**) and fully confluence (**C** and **D**) conditions were briefly treated with *C. perfringens* neuraminidase to remove preexisting sialic acids and then imaged for Core-1 O-glycans by ST3Gal1 using Alexa Fluor® 555 conjugated CMP-SA (red) and N-glycans by ST6Gal1 using Alexa Fluor® 488 conjugated CMP-SA (green). **A** and **B** are for the exact same viewing area. **C** and **D** are for the exact same viewing area. Cell nuclei were revealed with DAPI staining in blue in **B** and **D**. It is clear that N-glycans are expressed preferentially at peripheral positions, especially on protrusions of the cells, compared to Core-1 O-Glycans that are more centralized and evenly distributed on cells.

Figure 5. Mosaic sT Antigen Expression on HeLa cells. Confluent HeLa cells were imaged for sT antigen by ST6GalNAc4 with CMP-azido-SA and Alexa fluor® 555 via click chemistry (red). Nuclei were revealed in blue with DAPI. Intracellular contents were revealed by OGT with UDP-azido-GlcNAc and Alexa Fluor® 488 via click chemistry (green). Panel **A**, **B** and **C** are from a same viewing area. Cells marked with * and # are neighboring cells showing striking different intensities on sT antigen expression. A single positive cell surrounded by negative cells is circled in **B**.

Figure 6. Expression of sT antigen on a colony of HeLa cells that were derived from a single cell. A HeLa cell population was plated for single cell isolation and grown in DMEM medium (with 10% FBS) for 11 days at 37°C with 5% of CO_2 until a single colony formed in the well. The colony was imaged by ST6GalNAc4 with Alexa Fluor® 555 conjugated CMP-SA in red and countered imaged by OGT with UDP-azido-GlcNAc and Alexa Fluor® 488 in green. Nuclei were stained with DAPI in blue. The sT antigen positive cells are more abundant at the center compared to the edges of the colony. As the cells at the center of the colony were older and more crowded than the cells at the edges of the colony, this result suggests that the expression of sT antigen is age and stress dependent.

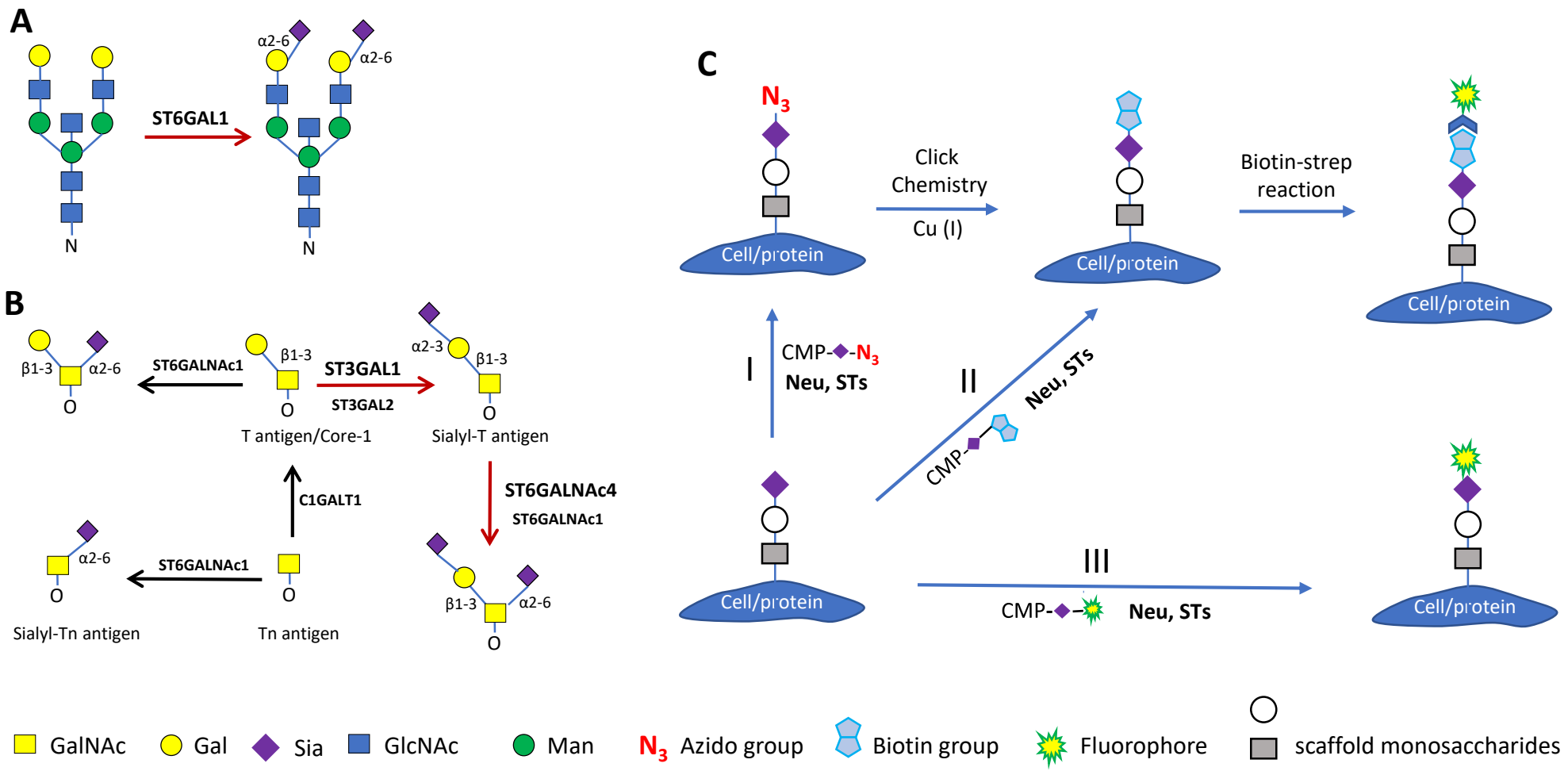

Figure 1. Sialylation reactions on N-glycans (A) and O-glycans (B) utilized in this report, and, methods of sialoglycan labeling (C). In **A** and **B**, sialylation reactions that are utilized in this report for labeling and imaging are indicated with red arrows. In **C,** three methods are depicted for sialoglycan labeling and imaging. In method I, azido-sialic acid is incorporated into sialoglycans, followed by click chemistry reaction to attach a biotin molecule and then labeled by fluorophore-conjugated streptavidin. In method II, biotinylated sialic acid is incorporated into sialoglycans and then labeled by fluorophore-conjugated streptavidin. Method III is named as Direct Fluorescent Glycan Labeling (DFGL) where sialoglycans are labeled by direct incorporation of fluorophore-conjugated sialic acid. Neu, neuraminidase; STs, sialyltransferases; CMP, cytidine monophosphate**.**

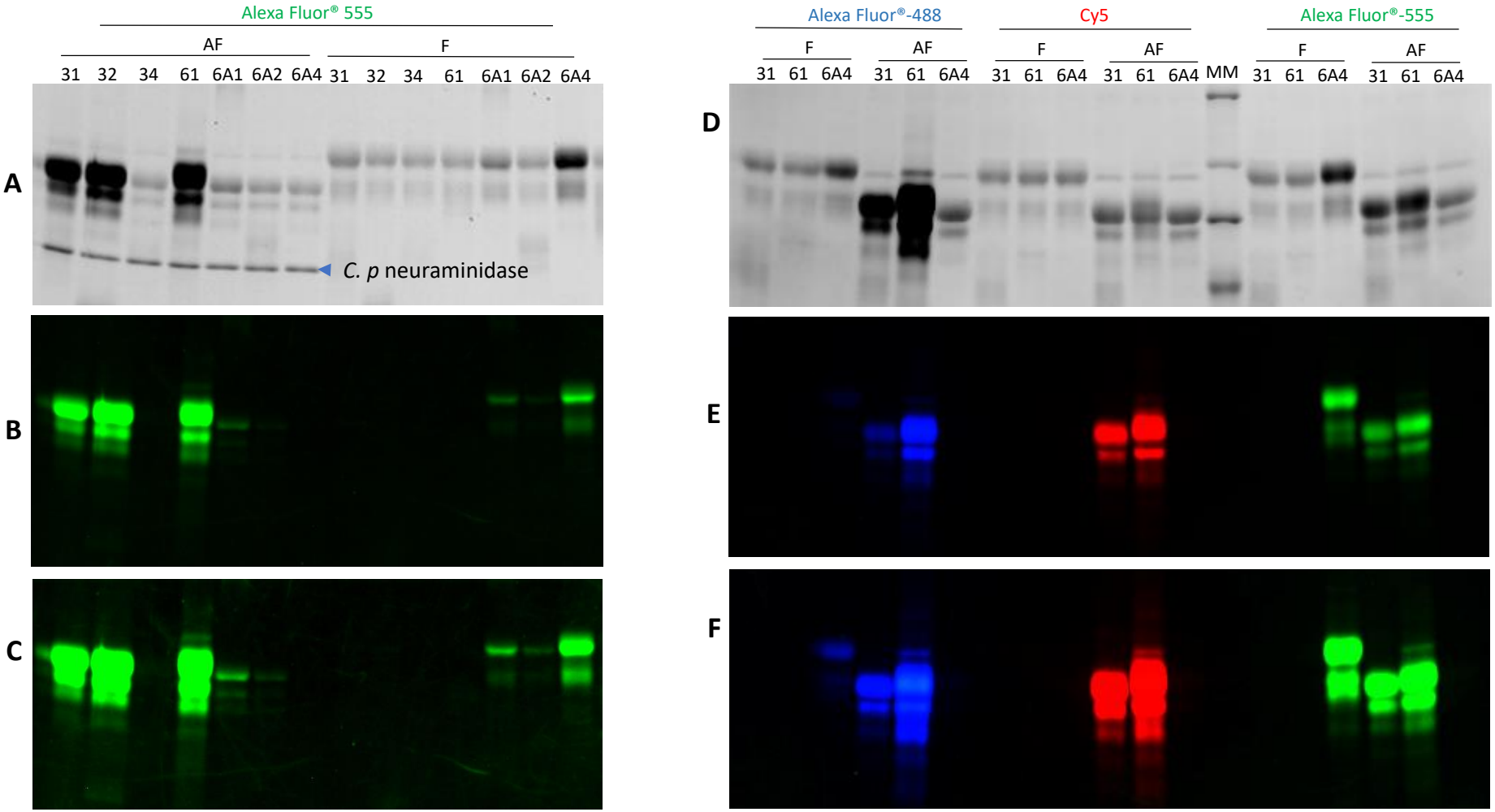

Figure 2. Fluorophore conjugated CMP-Sialic acids are tolerated by various sialyltransferases. A (TCE image), **B** and **C** (fluorescent images with different contrast) were images for a same SDS-PAGE gel, where Alexa Fluor® 555 labeled fetuin (F) or asialofetuin (AF) via indicated sialyltransferases was separated. **D** (TCE image), **E** and **F** (fluorescent images of different contrast) were images for a same SDS-PAGE gel, where Alexa Fluor® 488, 555 and Cy5 labeled F or AF with indicated sialyltransferases were separated. 31, ST3Gal1; 32, ST3Gal2; 34, ST3Gal4; 61, ST6Gal1; 6A1, ST6GalNAc1; 6A2, ST6GalNAc2; 6A4, ST6GalNAc4. Same amounts of F or AF (2.5 µg) was loaded into each lane in both **A** and **D**; however, due to the presence of multiple benzene rings in Alexa-Fluor® dyes, Alexa Fluor® 488 and 555 labeled proteins showed significantly increased band intensities in TCE gels. The *C.P neuraminidase* used for AF preparation in panel **A** was not removed, as it showed no glycosidase activity on the introduced orthogonal sialic acids. MM, molecular marker. Full-length gels are presented in Supplementary Fig. 1.

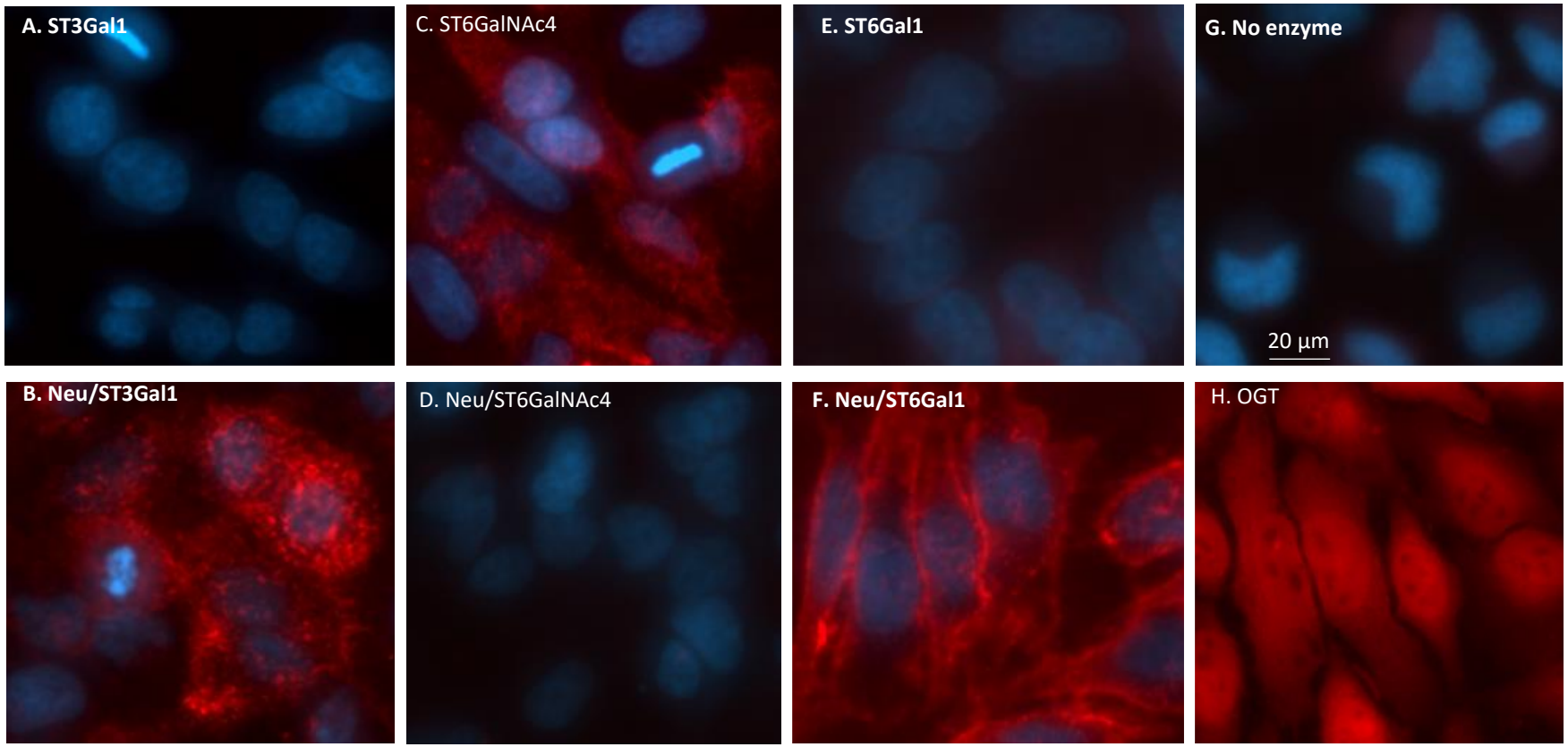

Figure 3. N- and O-glycans exhibit different localization on HeLa Cells. Confluent HeLa cells were imaged by ST3Gal1 (**A** and **B**), ST6GalNAc4 (**C** and **D**), ST6Gal1 (**E** and **F**) before (**A**, **C**, **E**) and after (**B**, **D, F**) *C.p. neuraminidase* treatment using CMP-azido-sialic acid. The cells were stained by ST3Gal1 and ST6Gal1 only after *C. perfringens* neuraminidase treatment, suggesting that both Core-1 O-glycan (T antigen) and N-glycan were highly sialylated on these cells. On the contrary, sT antigen was only stained by ST6GalNAc4 prior to *C. p* neuraminidase treatment (**C**). While sT antigen revealed in panels **B** and **C** evenly distributed on cell surface, N-glycans revealed in panel **F** showed a more peripheral localization. Additionally, not all cells in panel **B** and **C** were equally positive for sT antigen. For comparison, intracellular contents were stained by OGT in **H** using UDP-azido-GlcNAc. All staining was achieved through Alexa Fluor® 555 via click chemistry and streptavidin-biotin binding. Nuclei were stained in blue with DAPI.

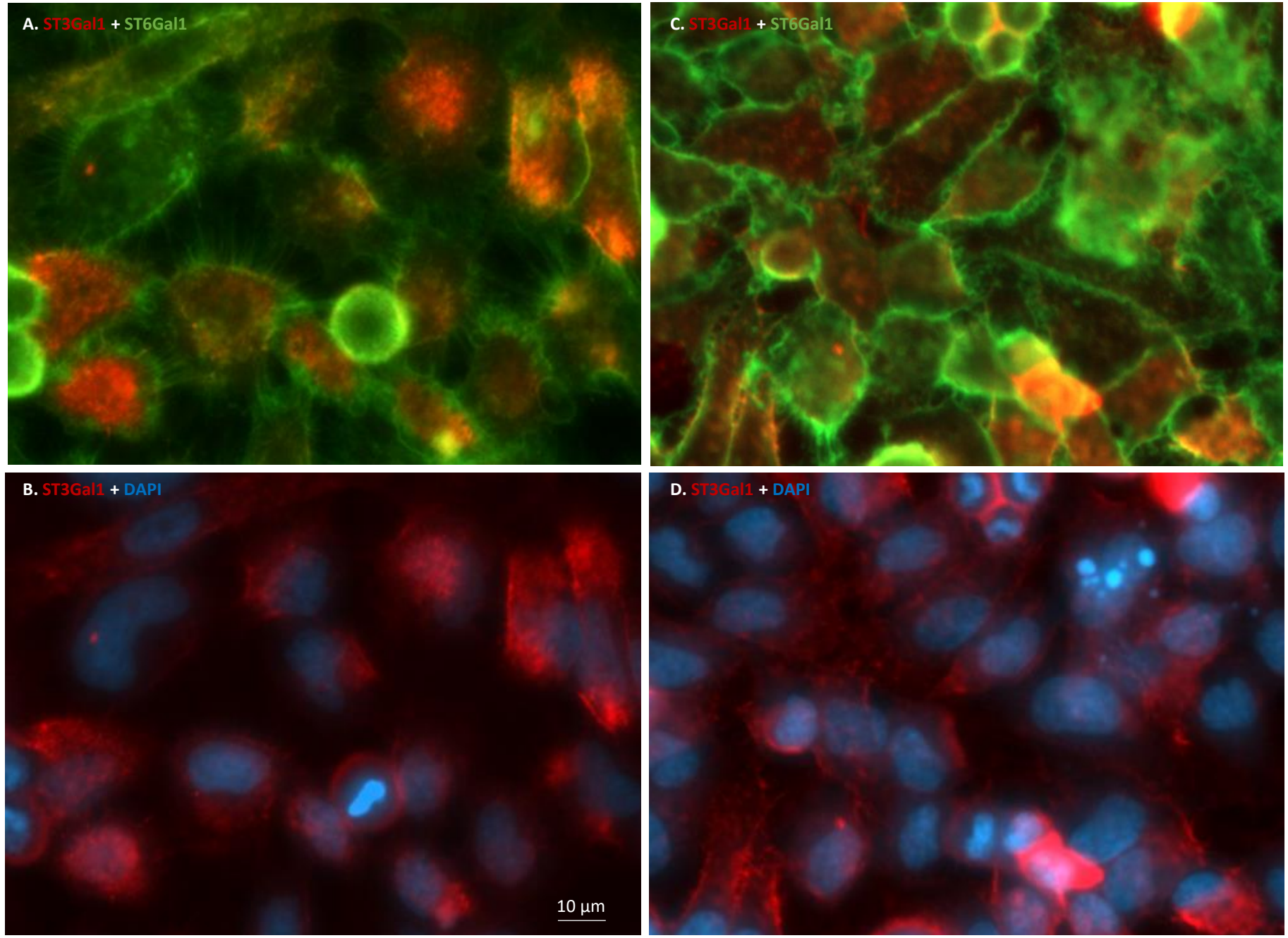

Figure 4. Differential Expression of N-glycans and Core-1 O-glycans Revealed by Double Imaging. HeLa cells at sub-confluence (**A** and **B**) and fully confluence (**C** and **D**) conditions were briefly treated with *C. perfringens* neuraminidase to remove preexisting sialic acids and then imaged for Core-1 O-glycans by ST3Gal1 using Alexa Fluor® 555 conjugated CMP-SA (red) and N-glycans by ST6Gal1 using Alexa Fluor® 488 conjugated CMP-SA (green). **A** and **B** are for the exact same viewing area. **C** and **D** are for the exact same viewing area. Cell nuclei were revealed with DAPI staining in blue in **B** and **D**. It is clear that N-glycans are expressed preferentially at peripheral positions, especially on protrusions of the cells, compared to Core-1 O-Glycans that are more centralized and evenly distributed on cells.

Figure 5. Mosaic sT Antigen Expression on HeLa cells. Confluent HeLa cells were imaged for sT antigen by ST6GalNAc4 with CMP-azido-SA and Alexa fluor® 555 via click chemistry (red). Nuclei were revealed in blue with DAPI. Intracellular contents were revealed by OGT with UDP-azido-GlcNAc and Alexa Fluor® 488 via click chemistry (green). Panel **A**, **B** and **C** are from a same viewing area. Cells marked with * and # are neighboring cells showing striking different intensities on sT antigen expression. A single positive cell surrounded by negative cells is circled in **B**.

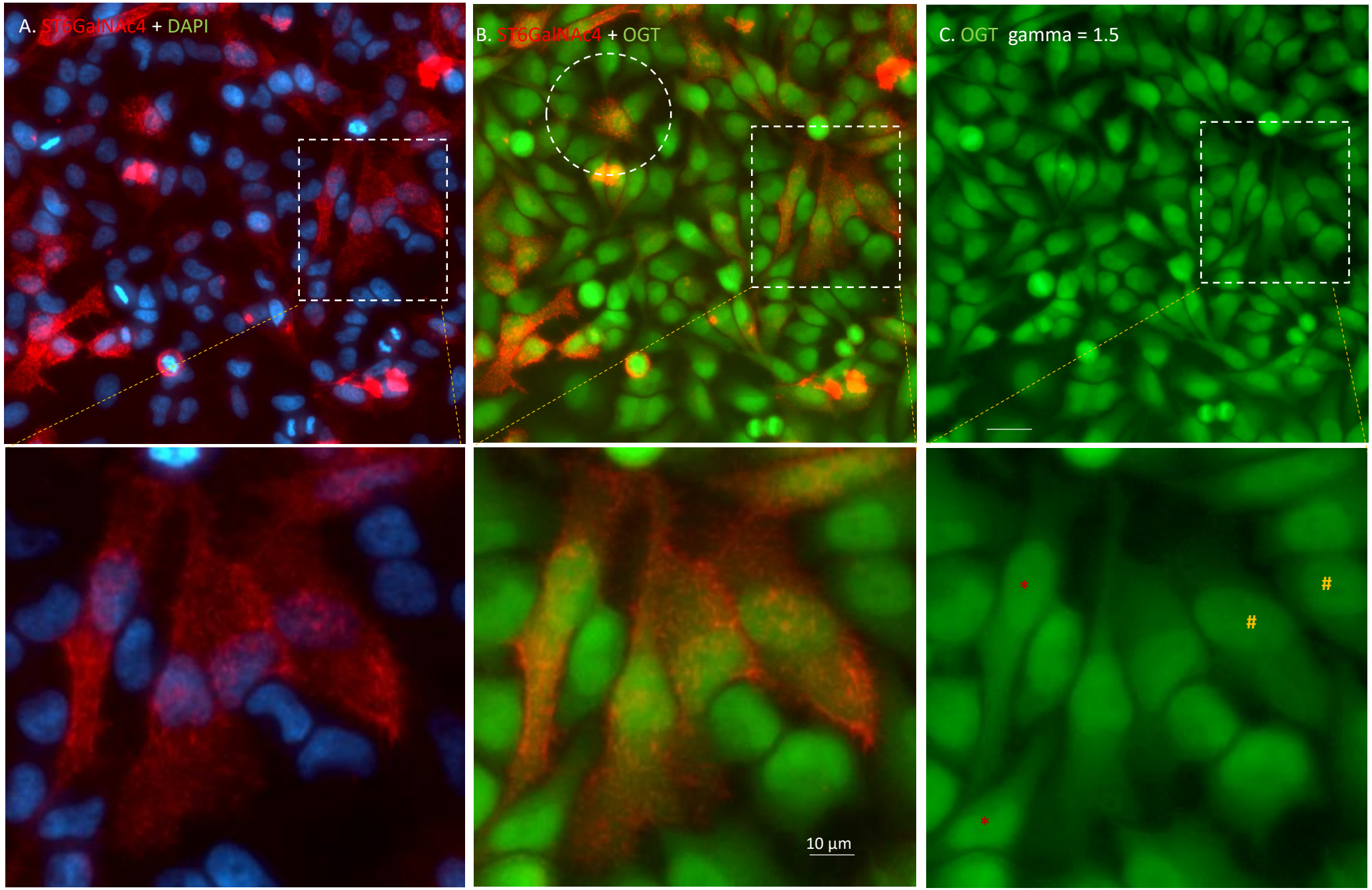

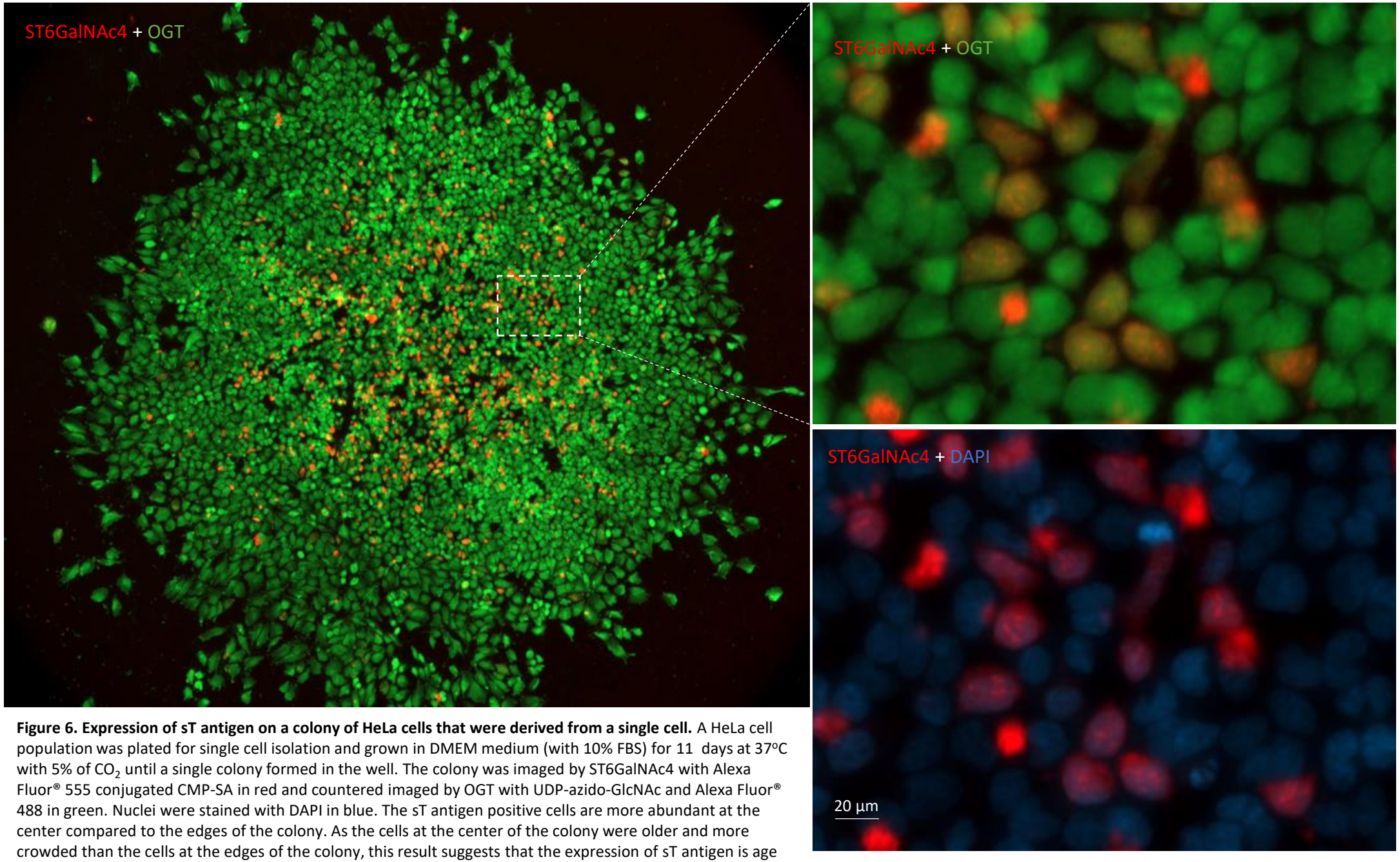

Figure 6. Expression of sT antigen on a colony of HeLa cells that were derived from a single cell. A HeLa cell population was plated for single cell isolation and grown in DMEM medium (with 10% FBS) for 11 days at 37ºC with 5% of CO_2 until a single colony formed in the well. The colony was imaged by ST6GalNAc4 with Alexa Fluor® 555 conjugated CMP-SA in red and countered imaged by OGT with UDP-azido-GlcNAc and Alexa Fluor® 488 in green. Nuclei were stained with DAPI in blue. The sT antigen positive cells are more abundant at the center compared to the edges of the colony. As the cells at the center of the colony were older and more crowded than the cells at the edges of the colony, this result suggests that the expression of sT antigen is age and stress dependent.